Primljen / Received: 5.2.2020.
Ispravljen / Corrected: 19.9.2020.
Prihvaćen / Accepted: 27.1.2021.
Dostupno online / Available online: 10.12.2021.

Influence of near-fault characteristics on inelastic response of multi-storey building with intensity measurement analysis

Authors:

Ali A. Muhsin, M.Sc. CE
Al-Nahrain University, Iraq
Faculty of Civil Engineering
aliabdulwahid80@gmail.com
Corresponding author

Assit.Prof. **Hussam K. Risan**, PhD. CE
Al-Nahrain University, Iraq
Faculty of Civil Engineering
dr.hussamrisan@gmail.com

Research Paper

Ali A. Muhsin, Hussam K. Risan

Influence of near-fault characteristics on inelastic response of multi-storey building with intensity measurement analysis

This study is presented to achieve three objectives: (1) to compare between the inelastic responses of buildings under near and far fault excitations, (2) to investigate the effect of the pulse to structural period ratio, and (3) to evaluate a set of intensity measurements (IMs) in terms of near fault (NF) earthquakes. A real reinforced concrete building with 35 storeys is analysed in the scope of the first and second objectives, whereas the third objective involves three general-frame buildings consisting of 6, 13, and 20 storeys. Results show that the NF excitation can drive the building to exceed its life safety performance level. Furthermore, the accuracy of the IM highly depends on the vibration period of the building and the function used to calculate the IM.

Key words:
near-fault earthquakes, inelastic response, pulse period, intensity measurement

Prethodno priopćenje

Ali A. Muhsin, Hussam K. Risan

Utjecaj karakteristika bliskih potresa na neelastični odziv višekatnice i analiza mjerenja intenziteta

Studija je izrađena kako bi se ostvarila tri cilja: (1) usporedba neelastičnih odziva građevina na bliske i udaljene pobude, (2) istraživanje utjecaja odnosa impulsnoga perioda i perioda konstrukcije te (3) ocjena niza mjerenja intenziteta (IM) za bliske potrese. Postojeća armiranobetonska zgrada s 35 katova analizira se u okviru prvoga i drugoga cilja, dok se u okviru trećega cilja analiziraju tri okvirne građevine s po 6, 13 i 20 katova. Rezultati pokazuju da kod bliske pobude može na građevinama doći do prekoračenja razine sposobnosti zaštite života. Osim toga, točnost mjerenja intenziteta u velikoj mjeri ovisi o periodu titranja građevine i o funkciji koja se rabi za izračunavanje vrijednosti IM.

Ključne riječi:
bliski potresi, neelastični odziv, impulsna perioda, mjerenje intenziteta

1. Introduction

Earthquakes occurring near the fault rupture have specific characteristics that distinguish them from ordinary ground motions recorded far from the source of rupture. An earthquake is classified as near-fault (NF) if it occurs in a region within 10–60 km of the fault [1]. NF earthquakes are identified by limited frequency and high amplitude pulse with a long duration that may or may not appear in the acceleration time history but is significantly evident in the velocity traces. The directivity and fling step are the most significant phenomena that affect the severity of NF earthquakes. The former causes a velocity pulse in the fault normal component, whereas the latter produces a step pulse in the displacement time history.

Previous studies have presented meaningful conclusions that help demonstrate NF earthquake characteristics. Ventura et al. [2] investigated the fling step effect on the nonlinear response of a tall building, which was modelled as an SDOF structure with different vibration periods and strength reduction factors. The results indicated that the response of structures depends on the ratio of rise time to the structural period. Moreover, the NF motions with the fling step effect have a severe effect on the tall building because ground motion with the fling step effect produces a response that is remarkably higher than that without the fling step effect.

The difference between the elastic response spectra of NF and far-fault (FF) earthquakes was determined by Anil K. Chopra and Chatpan Chintanapakdee [3]. Two groups of earthquakes, including 15 NF and 15 FF motions, were examined in terms of pseudo-acceleration, pseudo-velocity, and displacement linear response spectrum. In the case of NF motions, the acceleration- and displacement-sensitive regions are remarkably wider, whereas the velocity-sensitive region becomes narrower than those in FF motions. This effect increases the range of structures that respond in a stiff manner under NF earthquakes. A. Elsheikh and A. Ghobarah [4] explored the effect of pulse-like ground motions on the behaviour of stiff and flexible frames. Digital filters were applied to segregate the velocity pulse from geological noise. They found that the response of a flexible frame to filtered and unfiltered data is approximately identical. By contrast, in the case of stiff frames, a significant difference was observed between the actual and modified records. These results show that the behaviour of stiff frames is highly dominated by velocity pulse. Mahmood Hosseini et al. [5] examined the validity of provisions contained in IBC 2009 and ACI 318-2014 codes that should ensure the life safety performance level of frame buildings under NF earthquakes. A three-component nonlinear dynamic analysis was performed on five frame buildings of up to 16 storeys in height. The observations indicated that the provisions of the codes poorly predict the response of structures under NF excitations. Therefore, the NF excitation should be considered separately using an appropriate analysis method. The study also emphasized that the ordinary response spectrum factor method is outdated. Kourosh Talebi Jouneghani et al. [6] reviewed behaviour of a 2D model of a six-storey frame building under pulse-like motions. They indicated that the displacement due to NF excitation exceeded design requirements by 30 %. Moreover, the structures under NF motions require high ductility demands to withstand velocity pulse. Mohsen Kohrangi et al. [7] discussed the effect of the shape of the acceleration response spectrum for pulse-like motions on the response of the buildings. A set of earthquakes with and without pulse-like motions, with equivalent acceleration response spectrum shapes, was examined. They found that the severity of NF earthquakes cannot be predicted by the shape of the spectrum only, and that thorough investigation of the pulse properties, which have a major effect on the intensity of the ground motion, is important. Mohsen Gerami and Davood Abdollahzadeh [8] studied the effect of the near fault ground motion on the element and structure demand and capacity. They analysed 5 steel moment resistance frames under 20 near fault and far fault excitations by using nonlinear time history analysis. They found that the motions with long duration pulse magnified the axial force and flexural moment of the column and reduced the flexural strength and ductility capacity. Moreover, the bending demands of beams also increased due to the effect of near fault ground motions. Ghobarah [9] discussed how to idealize the pulse in near-fault records by finding the corresponding amplitude and period. For that he used 4 typical reinforced concrete frames excited by 4 near fault earthquakes. The nonlinear dynamic analysis was performed for actual records and equivalent velocity pulse. After comparison of response data, it was established that the behaviour of the long period structure is approximately the same for both types of excitation, whereas the results are almost different in the case of intermediate and short period structures. Previous studies have addressed a limited number of ground motions to investigate a specific case study, which normally leads to conditional results. Moreover, majority of existing investigations have used typical buildings with a 2D model that might not reflect the behaviour of complicated practical buildings. Hence, it is important to discuss the response of a real building to a wide range of NF earthquakes with various characteristics, such as fault mechanism, site condition, peak ground acceleration (PGA), and magnitude. The present study explores a large number of NF earthquakes with different properties to perform a comprehensive comparison between the behaviours of a real 3D practical building subjected to NF and FF records. Additionally, a statistical analysis is performed to assess a set of intensity measurements and evaluate their efficiency in measuring the severity of NF earthquakes.

2. Characterization of case study

Two cases were selected to fulfil the objectives of this study. The case study 1 is used to compare between the inelastic responses of buildings under near and far fault excitations, as well as to investigate the effect of the pulse to structural period ratio. The case is a real reinforced concrete hotel building constructed in Al Sharjah UAE consisting of 35 storeys with a total height of 135 m above ground level, and with the typical storey height of

Table 1. Properties of materials

Material property	Symbol	Value	Remarks
Compressive strength	$f_{ć}$	50 MPa	For case study 1, from ground floor to storey 20
Compressive strength	$f_{ć}$	40 MPa	For case study 1, from storey 21 to 35. For all frames in case study 2
Modulus of elasticity for concrete	E_c	$4500\sqrt{f_{ć}}$	For all elements
Modulus of elasticity for steel	E_s	200000 MPa	For all elements
Yielding Strength	f_y	460 MPa	For all elements
Concrete density	γ	25 kN/m^3	For all elements
Ultimate strain for concrete	ε_{cu}	0.003	For all elements

3.6 m. The building is vertically irregular, i.e. the height of the 1st storey is 4.65 m and that of the 18th and 32nd storeys is 5.2 m. The building plan dimensions are 31.3 m × 35.2 m. The building is designed to resist lateral loads with shear walls and cores distributed in the plan layout in an unsymmetrical pattern, as shown in Figure 1. The flat slab system is used in the building with beams on the external edges only. The slab thickness is 22 cm, except that at the 18th floor, where it amounts to 25 cm. The building is simulated as a 3D model in the SAP2000 software by using frame and shell elements, as shown in Figure 2. The ultimate compressive strength for all concrete members up to storey 20 is 50 MPa, whereas that of concrete used above storey 20 is 40 MPa.

By contrast, case study 2 is utilized to evaluate a set of intensity measurements (IMs) in term of near fault (NF) earthquakes. This case consists of typical frame buildings with 6, 13, and 20 storeys, and selected frames represent the short, moderate, and long period structures, respectively. The buildings are of an identical floor plan, which has a width of 6 m and 3 × 3 bays with a typical storey height of 3.6 m. Figure 3 shows the 3D model of the selected frames.

Material properties and constants of the studied cases are presented in Table 1. The studied buildings are examined under two load cases, namely, gravity and lateral earthquake loads. The vibrating mass source is selected to represent the critical case mentioned in ASCE 7-10, section 12.7, which includes the dead load, superimposed dead, and 25 % live loads. Table 2 lists the dead and live loads applied to the selected buildings.

Two types of elements were used to model the buildings in SAP2000. The beams, columns and shear walls are represented by a frame element with six degrees of freedom at each ends. The core wall and slab are modelled by using a shell element that has four joints and six degrees of freedom at each joint. Lateral loads are transferred by defining diaphragms at each storey level.

As the dimensions and properties of the sections are defined, the SAP2000 can automatically calculate the section capacity. Then the nonlinearity of the building can easily be defined by deriving the moment-curvature relation. Accordingly, the plastic hinges will be formulated at the sections where the applied load exceeds the section capacity. Knowing that, the positions of the plastic hinges are assumed to be at the ends of beams and columns.

The stiffness of the columns, beams, shear walls and slab are reduced to 0.7, 0.35, 0.35, and 0.25, respectively, to consider the cracking of the elements. The constant modal damping with a value of 0.05 is used for all modes.

Modal analysis is performed on the 3D models of the buildings by considering the vibration of six degrees of freedom, including three translations and three rotations with respect to the global direction axes. This study adopts 12 mode shapes, which satisfy the required accuracy. Table 3 indicates the mode shape characteristics of the building.

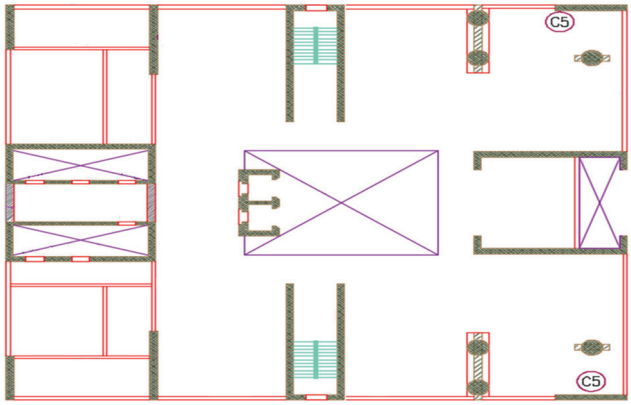

Figure 1. Framing layout

Table 2. Applied loads

Load	Case study 1	Case study 2
Typical live load [kN/m^2]	2	2.5
Live load for storey 18th [kN/m^2]	10	-
Typical superimposed dead load [kN/m^2]	3.2	1.68
Superimposed dead load for storey18th and 32nd	3.4	-

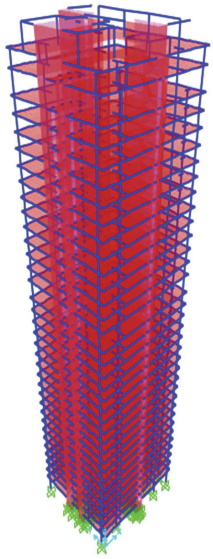

Figure 2. 3D View in SAP2000 (case study 1)

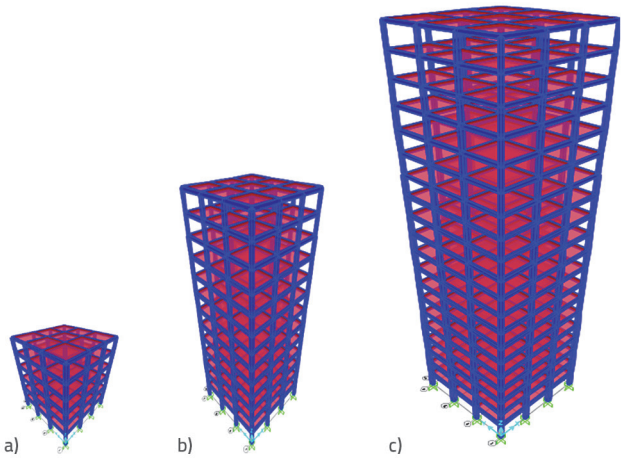

Figure 3. 3D View in SAP2000 (case study 2): a) 6 storeys; b) 13 storeys; c) 20 storeys

Table 3. Elastic periods in seconds

Mode shape No.	No. of storeys			
	35	6	13	20
1	6.84	0.93	2.18	3.42
2	4.77	0.93	2.18	3.42
3	3.92	0.82	1.91	2.94
4	1.56	0.29	0.73	1.23
5	1.13	0.29	0.73	1.23
6	1.03	0.26	0.64	1.09
7	0.67	0.15	0.42	0.73
8	0.49	0.15	0.42	0.73
9	0.44	0.13	0.37	0.65
10	0.38	0.09	0.28	0.51
11	0.28	0.09	0.28	0.51
12	0.28	0.08	0.25	0.46

3. Building behaviour

This section clarifies the difference in the response of a 3D practical multistorey RC wall building under NF and FF earthquakes with identical PGAs. The behaviour of the building is evaluated in accordance with the provisions stated in FEMA 356 [10], which classifies the limit state into three performance levels, namely, immediate occupancy, life safety, and collapse prevention. These levels are divided on the basis of the drift ratio during the elastic and inelastic states. Table 4 lists the limits for concrete wall buildings.

3.1. Earthquake excitation

Earthquake records, including many parameters, can considerably affect the structural response, such as the fault mechanism and ground motion magnitude. To eliminate the influence of these factors and keep focusing on the pulse

Table 4. Drift ratio limitation for concrete wall buildings according to FEMA 356

Drift ratio	Limit State		
	Immediate Occupancy (IO)	Life Safety (LS)	Collapse Prevention (CP)
Transient	0.5 %	1 %	2 %
Permanent	-	0.5 %	2 %
IO - Immediate Occupancy, LS - Life Safety, CP - Collapse Prevention			

Table 5. Properties of selected earthquakes

Earthquake	Station	Type	M1	Rrup2 [km]	Duration [s]
Northridge, 1994	Newhall - Fire Sta.	NF	6.69	05.92	15
Northridge, 1994	Anaheim - W Ball Rd	FF	6.69	68.62	20
Kobe, 1995	Port Island	NF	6.90	03.31	20
Kobe, 1995	Chihaya	FF	6.90	49.91	30
M1 - Earthquake moment magnitude, Rrup2 - Closest distance to the fault plane, NF - Near fault, FF - Far fault					

effect, the NF and FF records were selected for the same earthquake event. Two earthquakes are selected from the Pacific Earthquake Engineering Research (PEER) ground motion database to evaluate the behaviour of the building [11]. The selected earthquake events are 1994 Northridge, USA, and 1995 Kobe, Japan. Table 5 presents detailed properties of the selected earthquakes. These earthquakes are scaled to 0.3 g and are used to excite the building in the X direction.

3.2. Nonlinear analysis

Nonlinear analysis defines plastic hinges at both ends of beams and columns. The ultimate capacity of plastic hinge is assumed to be reached when the concrete strain at the extreme fibre is equal to 0.003. Figure 4 presents comparison of the maximum absolute drift ratio and the allowable drift ratios recommended by FEMA 356. Both FF cases are below the code limitations, whereas the NF records pass the LS performance level with maximum percentage differences of 30 % and 108 % in Northridge and Kobe ground motions, respectively. Figure 5 illustrates each storey's ductility demand, which is defined as the ratio of the maximum nonlinear interstorey drift to the maximum drift among overall storeys when the first plastic hinge occurs [12]. The average ductility demands produced by Northridge are 8.5 and 4.3, whereas the Kobe earthquake causes large ductility demands of 22.5 and 4.4 in the NF and FF cases, respectively.

The shear force is adopted by monitoring behaviour of the shear wall five (C5). Figure 6 plots the maximum shear force demand for the shear wall five (C5) with respect to the shear section capacity. The Northridge earthquakes have the maximum demands of 3,879 and 3,592 kN, whereas Kobe records produced 5,312 and 2,324 kN in the NF and FF cases, respectively. The applied shear forces at the bottom and top storeys are higher than the shear strength of the section, except in the case of FF Kobe. Thus, the critical capacities to demand ratios are 81 %, 77 %, and 54 % for NF Northridge, FF Northridge, and NF Kobe, respectively.

Figure 7 shows the maximum applied moment relative to the yield and plastic moment capacity for C5. The maximum values of the moment are 22,647 and 12,588 kNm in NF and FF Northridge cases, respectively, and 33,482 and 11,510 kNm in NF and FF Kobe, respectively. The applied moment exceeds the yield and plastic moment in many locations along the height of the designated shear wall.

Figure 8 depicts variation of roof displacement with time. The Northridge earthquake produced maximum displacements of 42.4 and 19.5 cm in the NF and FF cases, respectively, whereas Kobe ground motion caused maximum displacements

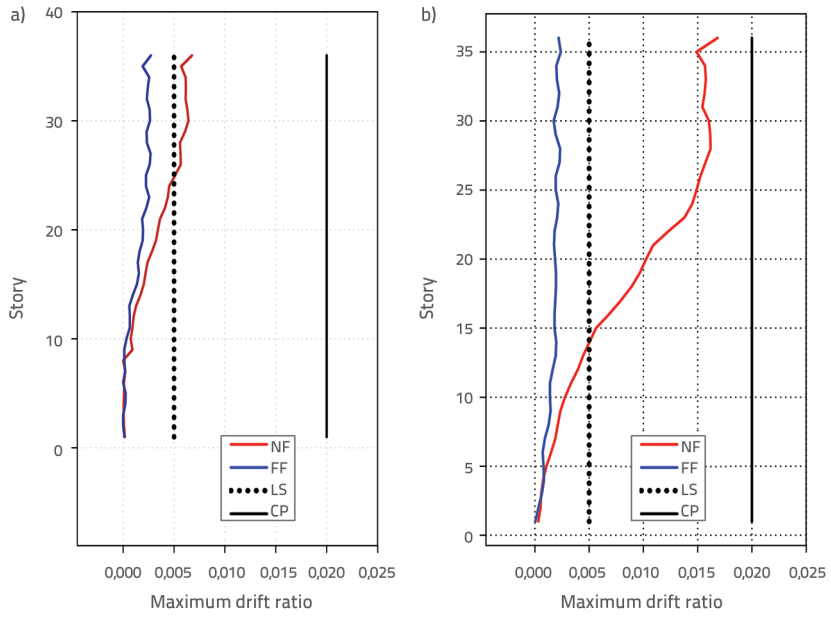

Figure 4. Maximum inelastic storey drift ratio: a) Northridge, max. drift ratio; b) Kobe, max. drift ratio

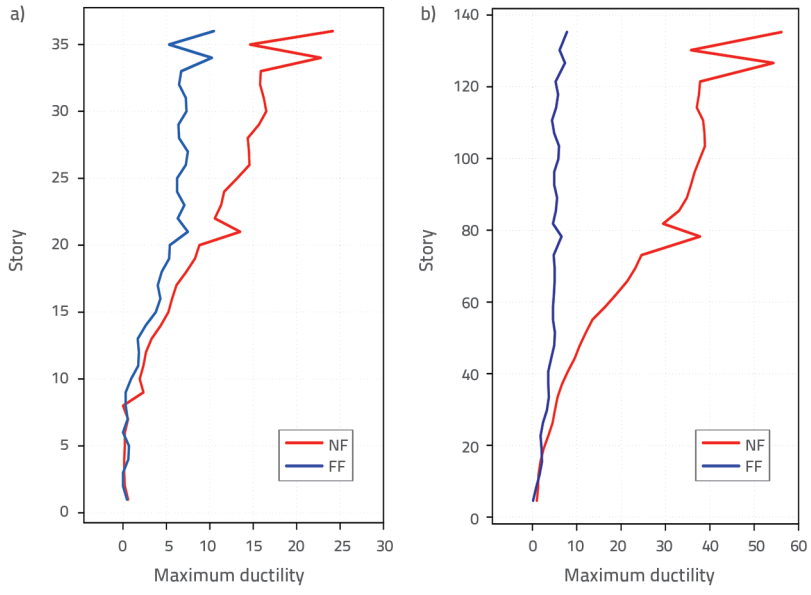

Figure 5. Maximum ductility demands: a) Northridge, max. ductility; b) Kobe, max. ductility

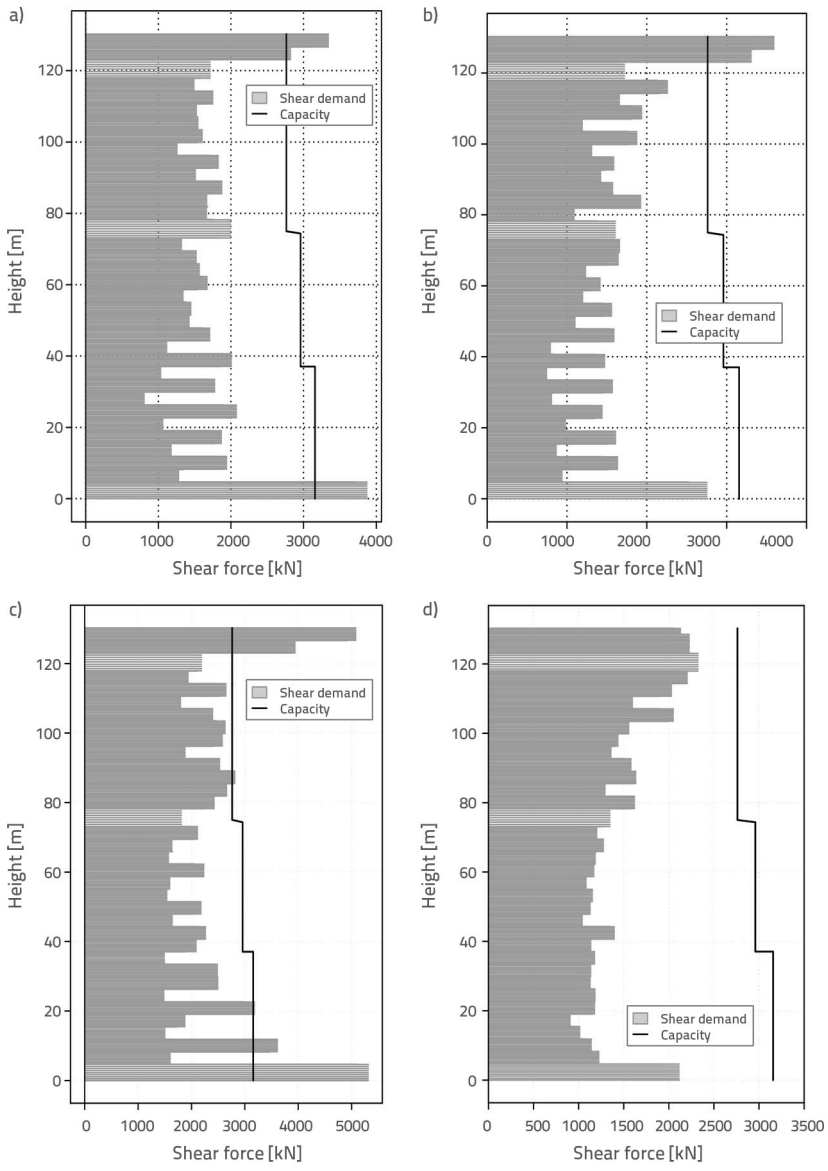

Figure 6. Maximum shear force applied to shear wall 5: a) NF Northridge, max. shear force; b) FF Northridge, max. shear force; c) NF Kobe, max. shear force; d) FF Kobe, max. shear force

of 121.8 and 22.3 cm for NF and FF cases, respectively. In the case of NF records, the maximum roof displacement occurred earlier than that of FF records, indicating that the effect of the high input energy occurring at the beginning of NF earthquakes is due to the directivity effect.

Table 6 summarizes the number and states of plastic hinges at the end of each earthquake with respect to the FEMA 356 limit states. The total numbers of plastic hinges produced by Northridge earthquake are 811 and 584 in the NF and FF cases, respectively, whereas those by Kobe are 1206 and 627 in the NF and FF cases, respectively.

Hence, NF ground motions produce larger response and strength demands than FF earthquakes although both earthquakes have identical magnitudes and PGAs.

The comparison of the linear behaviour and the nonlinear response of the building is shown in Table 7. In the case of strong ground motion, such as NF Kobe, which exceeds the code limitations for interstorey drifts, the nonlinear analysis obtains a response higher than that of linear approaches. This finding indicates that the strong ground motions cause a considerable reduction in the overall stiffness of the building after it reaches the yielding limit. This reduction is ignored in linear analysis, which assumes that the structure can maintain its initial stiffness to the end of vibration.

Table 6. Summary of the number and status of plastic hinges

Earthquake	IO	IO-LS	LS-CP	> CP	Total
NF Northridge	786	0	0	25	811
FF Northridge	571	1	0	12	584
NF Kobe	779	213	0	214	1206
FF Kobe	618	0	0	9	627

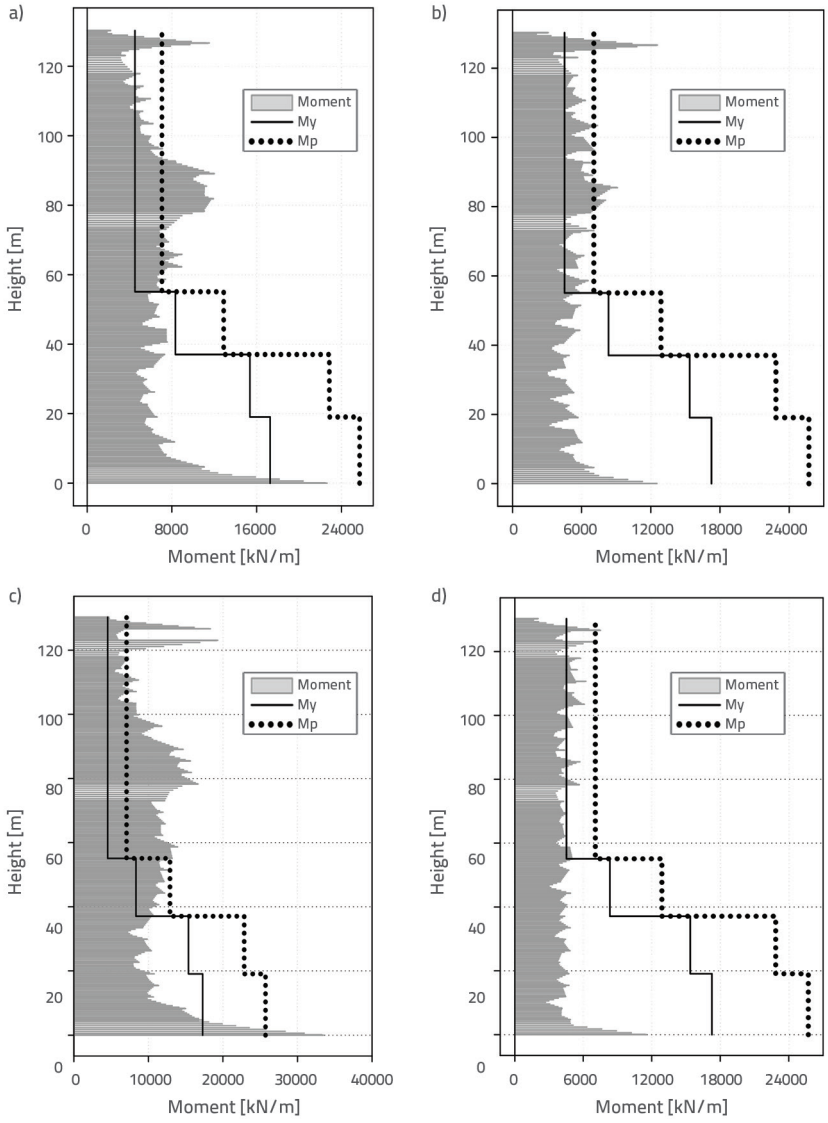

Figure 7. Maximum inelastic moment around Y axis applied to shear wall 5: a) NF Northridge, max. moment; b) FF Northridge, max. moment; c) NF Kobe, max. moment; d) FF Kobe, max. moment

4. Pulse period

The pulse period in NF records has a major influence on the behaviour of structures [1]. Building response increases as the ratio of pulse period to the structural period (Tp/T1), approach 1. To verify this result with respect to an actual building under 3D analysis, the selected case study (case study 1) is examined under two records for identical earthquakes with two pulse periods. The 1992 Landers, California, earthquake, is selected to perform this investigation. Two records were selected, namely, Yermo Fire Station and Barstow, which have (Tp/T1) ratios equal to 1.09 and 1.30, respectively. These records were selected to examine two conditions, i.e. (Tp/T1) approach 1 and larger than 1. Table 8 presents properties of the selected records. The nonlinear response is evaluated for both records under identical PGAs scaled to 0.3 g.

Figure 9 shows the maximum drift ratio with respect to the allowable drift ratio limits stated in FEMA 356. Both records considerably pass the LS performance level with maximum percentage differences of 66 % and 33 % for Yermo Fire Station and Barstow records, respectively. Maximum ductility demands are calculated and presented in Figure 10. Ductility demands have several jumps through the building height due to the presence of the soft storey. However, the average ductility demands are 17.7 and 15.4 for Yermo Fire Station and Barstow records, respectively.

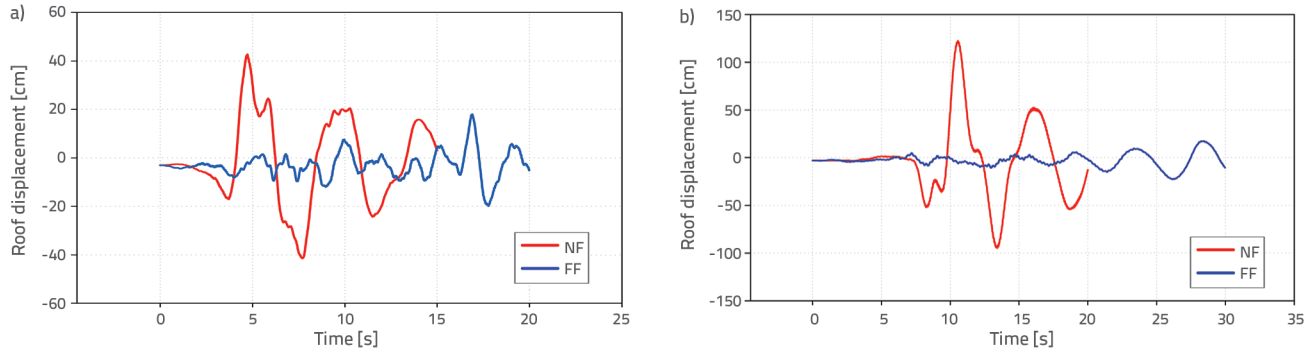

Figure 8. Time history of inelastic roof displacement: a) Time history of inelastic roof displacement; b) Time history of inelastic roof displacement

Table 7. Summary of studied parameters

Earthquake	Max. roof displacement [cm]		Max. drift ratio		Max. shear force [kN]		Max. moment [kNm]		Average ductility
	Linear	Nonlinear	Linear	Nonlinear	Linear	Nonlinear	Linear	Nonlinear	Linear
NF North	50.6	42.4	0.007	0.006	1966	3879	19126	22647	8.5
FF North	18.2	19.5	0.003	0.002	1288	3592	11349	12588	4.3
NF Kobe	117.4	121.8	0.014	0.016	2078	5312	22549	33482	22.5
FF Kobe	22.7	22.3	0.002	0.002	495	2324	4553	11510	4.4

Table 8. Records properties

Items	Station	M	Rrup [km]	Tp	Tp/T1
Landers	Yermo Fire Station	7.3	23.6	7.5	1.09
	Barstow		34.9	8.9	1.3

Figure 11 presents the shear force diagram of C5 with respect to the section shear capacity. Maximum shear demands are 3,909 and 2,414 kN for Yermo Fire Station and Barstow records, respectively. The shear demand imposed by Yermo Fire Station becomes greater than the shear strength in several points with a critical capacity-to-demand ratio of 70 %. Figure 12 shows the moment distribution over the height of C5 around the global Y-axis with respect to the yield and plastic moment limits. Both cases produce a moment larger than the yield limit. However, the maximum moments caused by Yermo Fire Station and Barstow are 33,185 and 20,654 kN·m, respectively. Figure 13 plots the time history of inelastic roof displacement, which demonstrates that the Yermo Fire Station and Barstow cause maximum displacements equal to 110.3 and 85.3 cm, respectively.

Table 9 shows the number and states of plastic hinges obtained at the end of both earthquakes with respect to each performance level in accordance with FEMA 356 recommendations. The results clearly show that Yermo Fire Station causes a considerably larger damage at 65 plastic hinges with the collapse prevention state compared to the Barstow motion at 15 plastic hinges. Table 10 briefly compares linear and nonlinear responses of the building under pulse-type earthquakes.

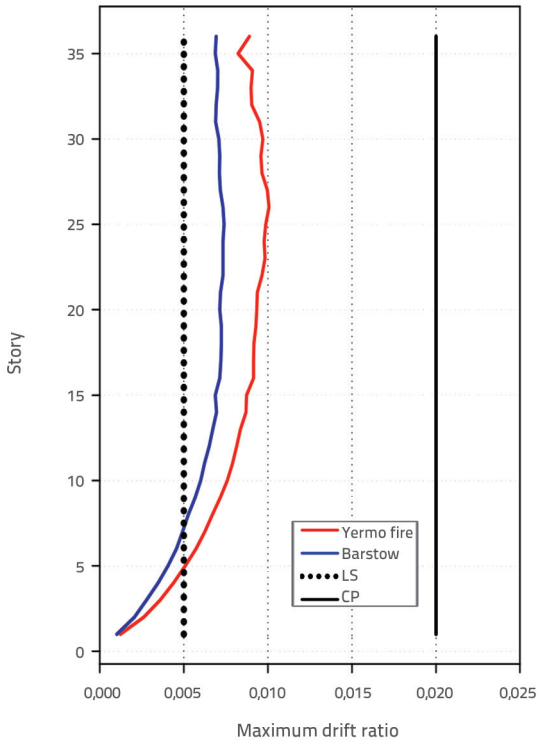

Figure 9. Maximum inelastic storey drift ratio

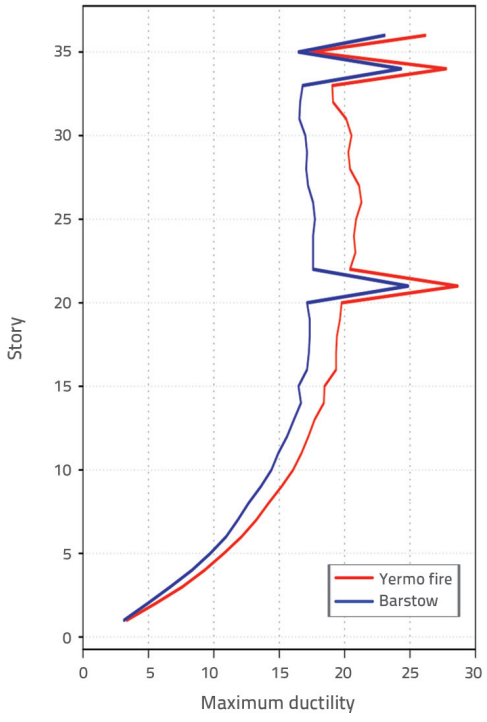

Figure 10. Maximum ductility

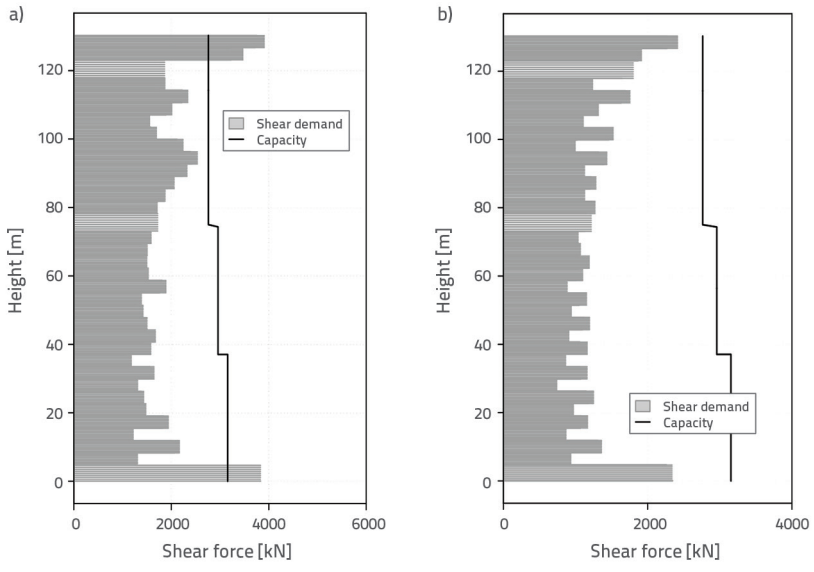

Figure 11. Maximum inelastic shear force: a) Yermo Fire Station, max shear force; b) Barstow, max shear force

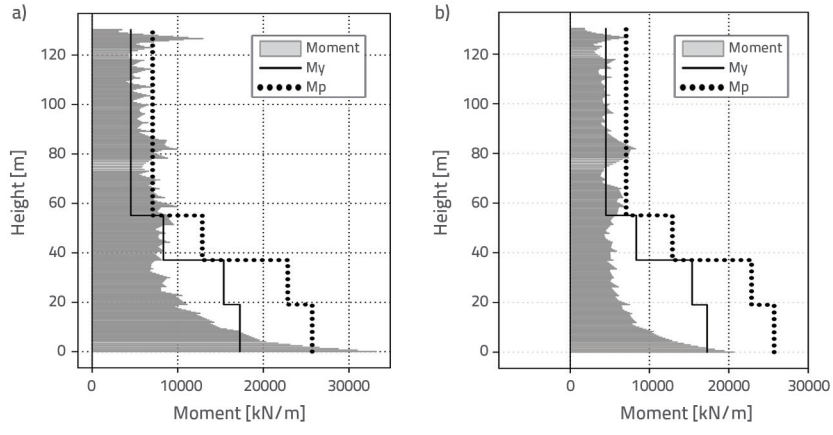

Figure 12. Maximum inelastic moment: a) Yermo Fire Station, max moment; b) Barstow, max moment

5. Intensity measurements

IM is an indicator of earthquake severity that can predict structural damage imposed by the ground motion. The PGA is a widely used parameter for the assessment of earthquake severity. Although seismic codes use PGA to measure the design strength, measuring the intensity of NF earthquakes is inefficient. Accordingly, researchers have attempted to develop sufficient parameters that can measure the damage potential of strong earthquakes. This section aims to investigate the efficiency of the proposed IMs and whether they can accurately describe the response of the RC building under NF earthquakes. Six parameters were selected, namely, arise intensity (AI), specific energy density (SED), cumulative absolute velocity (CAV), maximum incremental velocity (MIV), acceleration spectrum intensity (ASI), and velocity spectrum intensity (VSI). These parameters can be classified into three groups, namely, energy (AI, SED), velocity (CAV, MIV), and spectrum (ASI, VSI) measurements. The selected IM can be defined as follows:

$$AI = \frac{\pi}{2g}\int_0^{t_d}\left[a(t)\right]^2 dt \quad (1)$$

$$SED = \int_0^{t_d}\left[v(t)\right]^2 dt \quad (2)$$

Table 9. Summary of the number and status of plastic hinges

Earthquake	IO	IO-LS	LS-CP	> CP	Total
Yermo Fire Station	868	51	0	65	984
Barstow	817	1	0	15	833

Table 10. Summary of studied parameters

Items	Max. roof displacement [cm]		Max. drift ratio		Max. shear force [kN]		Max. moment [kN.m]		Average ductility
	Linear	Nonlinear	Linear	Nonlinear	Linear	Nonlinear	Linear	Nonlinear	Nonlinear
Yermo Fire Station	102	108.5	0.01	0.01	1964	3830	19231	33185	17.7
Barstow	80.5	83.6	0.008	0.007	1404	2346	14390	20654	15.4

$$CAV = \int_0^{t_d} |a(t)| dt \quad (3)$$

$$ASI = \int_{0\,1}^{0.5} S_a(t) dt(\xi = 0{,}05) \quad (4)$$

$$VSI = \int_{0\,1}^{2.5} S_v(t) dt(\xi = 0{,}05) \quad (5)$$

where is the total duration of the earthquake; and are the instantaneous acceleration and velocity records, respectively; and and are the instantaneous acceleration and velocity spectrum data, respectively. MIV can be defined as the maximum area under the velocity time history between points of zero velocity [13].

A set of 90 NF earthquakes was selected from the PEER ground motion database. The selected records are mentioned in the technical report for the PEER ground motion database as normal fault pulse-like ground motions [14]. These data have a magnitude ranging from 5 to 7.6, and the closest distance to the fault plane varies from 0.1 km to 74.3 km.

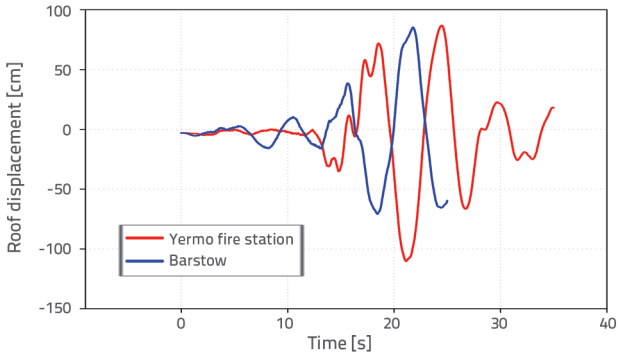

Figure 13. Time history of inelastic roof displacement

The nonlinear time history analysis is conducted for each building (case study 2) under 90 earthquake excitations with a unique PGA (0.3g); hence, the total number of studied cases are 270. IM is performed by testing the correlation between these measurements and the maximum roof displacement, maximum interstorey drift, and maximum base shear. The Pearson linear correlation coefficient is adopted to assess the relations between the examined variables. The relations are described as perfect, strong, moderate, weak, and none, depending on the value of the correlation coefficient.

Figures 14-16 summarize the correlation coefficient results between the selected IM and maximum roof displacement, maximum interstorey drift, and maximum base shear, respectively. The correlation of identical IMs varies for the same building with respect to response parameters. Consequently, the maximum roof displacement of the six-storey frame obtains the highest correlation for all IMs. The correlation of maximum roof displacement is consistent with the maximum base shear for the 13-storey building. However, the maximum base shear of the 20-storey frame has a predominating correlation throughout the studied IMs.

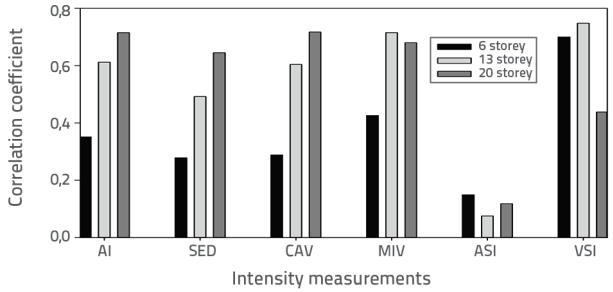

Figure 14. Maximum roof displacement correlation coefficient

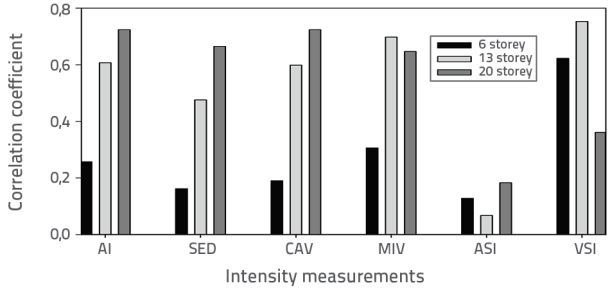

Figure 15. Maximum inter-storey drift correlation coefficient

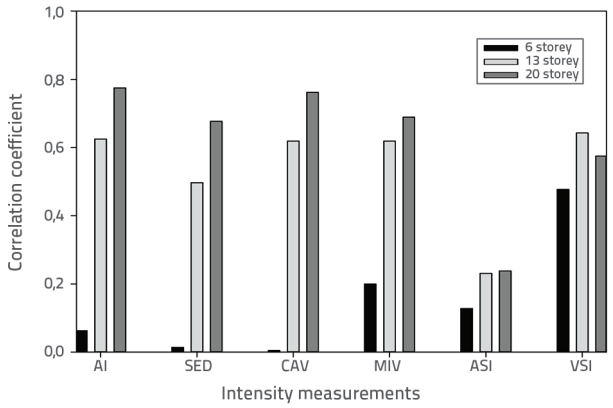

Figure 16. Maximum base shear correlation coefficient

Although AI and SED are based on the energy measurement, AI obtains the highest correlation among all the examined buildings. The reason may be that the AI determines the energy directly from the acceleration time history, whereas SED determines the energy from the integrated acceleration time history. Furthermore, the comparison between IMs based on velocity, namely, MIV and CAV, shows that MIV obtains a high correlation in the 6- and 13-storey buildings, whereas CAV produces strong relations in the 20-storey building. The IM results depending on the response spectrum (ASI and VSI) show that VSI is the most accurate IM in calculating the response of short- and moderate-period buildings. However, ASI produces the weakest correlation among all the studied IMs because ASI focuses on the intensity of the response spectrum between 0.1

s and 0.5 s, which is outside of the studied periods, whereas VSI measures the intensity between 0.1 s and 2.5 s, which is within the range of the 6- and 13-storey buildings. The 6-storey building has the weakest correlation with IM, except for VSI because the response of short-period structures is controlled by the acceleration-sensitive region of the response spectrum, which significantly varies with respect to the examined earthquake.

6. Conclusions

This study highlights an important scope in the seismic structural engineering field, that is, the special properties of NF earthquakes and their effects on the inelastic response of multistorey RC buildings. Several cases have been investigated, including a practical RC multistorey building and a set of general-frame buildings. A large number of NF earthquakes have been used to cover a wide range of ground motion characteristics. A 3D time history analysis is adopted to evaluate the linear and nonlinear dynamic behaviours of interesting cases. The conclusions and recommendations are listed as follows:

- NF ground motions produce larger response and strength demands than FF earthquakes although both earthquakes have identical magnitudes and PGAs. The value of PGA is inadequate to measure intensity of NF earthquakes. Consequently, the buildings designed using the traditional method, which is based on the acceleration spectrum, cannot sufficiently resist the pulse imposed by NF ground motions.
- The results of the performance level evaluation for a 35-storey practical building under NF and FF earthquakes prove that the NF excitation can significantly exceed the life safety level.
- The soft storey has a noticeable effect on the behaviour of the 35-storey building under NF and FF ground motions, leading to a large jump in the interstorey drift and ductility demand curves.
- The pulse period of the ground motion highly controls behaviour of the building, wherein the response is expected to be large, as the ratio of the pulse period to the vibration period of the building approaches unity.
- The evaluation of IMs in terms of earthquake energy indicates that the AI is more accurate than the SED. This conclusion is applicable for all the examined buildings, including buildings with 6-, 13-, and 20-storey frames.
- The comparison between MIV and CAV shows that MIV is suitable for 6- and 13-storey buildings, whereas CAV produces high accuracy in 20-storey buildings.
- The assessment of ASI and VSI demonstrates that VSI has an accurate IM in predicting the response of short- and moderate-period buildings, whereas ASI produces a poor correlation among all studied IMs.
- IMs are poor predictors of the response of short-period structures, which lies within the acceleration-sensitive region of the earthquake.

REFERENCES

[1] Heydari, M., Mousavi, M.: The comparison of seismic effects of near-field and far-field earthquakes on relative displacement of seven-storey concrete building with shear wall, Current World Environment, 10 (2015) 1, pp. 0-46, https://doi.org/10.12944/cwe.10.special-issue1.07.

[2] Ventura, C.E., Archila, M., Bebamzadeh, A., Liam Finn, W.D.: Large coseismic displacements and tall buildings, The Structural Design of Tall and Special Buildings, 20 (2011), pp. 85-99, https://doi.org/10.1002/tal.739.

[3] Anil, K., Chintanapakdee, C.: Comparing response of SDF systems to near-fault and far-fault earthquake motions in the context of spectral regions, Earthquake Engineering and Structural Dynamics, 30 (2001) 12, pp. 1769-1789, https://doi.org/10.1002/eqe.92.

[4] Elshikh, A., Ghobarah, A.: Response of RC structures to near-fault records, Emirates Journal for Engineering Research, 9 (2004) 2, pp. 45-51.

[5] Hosseini, M., Hashemi, B., Safi, Z.: Seismic design evaluation of reinforced concrete buildings for near-source earthquakes by using nonlinear time history analyses, Procedia Engineering, 199 (2017), pp. 176–181, doi: 10.1016/j.proeng.2017.09.225.

[6] Jouneghani, K., Hosseini, M., Rohanimanesh, M., Dehkordi, M.: Evaluation main parameters effects of near-field earthquakes on the behaviour of concrete structures with moment frame system, Advances in Science and Technology Research Journal, 11 (2017) 3, pp.10–23, https://doi.org/10.12913/22998624/74135.

[7] Kohrangi, M., Vamvatsikos, D., Bazzurro, P.: Pulse-like versus non-pulse-like ground motion records: spectral shape comparisons and record selection strategies, Earthquake Engineering & Structural Dynamics, 48 (2019) 1, pp. 46-64, https://doi.org/10.1002/eqe.3122.

[8] Gerami, M., Abdollahzadeh, D.: Local and global effects of forward directivity, GRAĐEVINAR, 65 (2013) 11, pp. 971-985, https://doi.org/10.14256/JCE.908.2013.

[9] Ghobarah, A.: Response of structures to near-fault ground motion.13th World Conference on Earthquake Engineering Vancouver, B.C., Canada. 2004.

[10] FEMA 356: Prestandard and Commentary for The Seismic Rehabilitation of Buildings, Federal Emergency Management Agency, 2000.

[11] PEER: Pacific Earthquake Engineering Research Center, Strong Motion Database, http://peer.berkeley.edu, 2018.

[12] Annan, C.D., Youssef, M.A., El Naggar, M.H.: Seismic vulnerability assessment of modular steel buildings, Journal of Earthquake Engineering, 13 (2009) 8, pp. 1065-1088, https://doi.org/10.1080/13632460902933881.

[13] Ozmen, H.B., Inel, M.: Damage potential of earthquake records for RC building stock, Earthquakes and Structures, 10 (2016) 6, pp.1315-1330, http://dx.doi.org/10.12989/eas.2016.10.6.1315.

[14] California Geological Survey-Strong Motion Instrumentation Program (CGS-SMIP) and (PEER), Technical Report for the PEER Ground Motion Database, beta version, October 2010.

[15] Chopra, K., Anil, Ch.: Dynamics of Structures: Theory and Applications to Earthquake Engineering, Vol. 3. Upper Saddle River, NJ: Pearson/Prentice Hall, https://doi.org/10.1061/(asce)0733-9445133:5(752), 2007.

[16] Paz, M., Leigh, W.: Structural Dynamics Theory and Computation, Fifth Edition, Kluwer Academic Publisher, Boston/ London, 2004.

[17] Clough, R., Penzien, J.: Dynamics of Structures, Third Edition, Computers & Structures, Inc., United States of America, 2003.